

Contact angles by the solid-phase grain boundary wetting (coverage) in the Co–Cu system

B. B. Straumal · O. A. Kogtenkova ·
A. B. Straumal · Yu. O. Kucheyev ·
B. Baretzky

Received: 15 November 2009 / Accepted: 2 March 2010 / Published online: 18 March 2010
© Springer Science+Business Media, LLC 2010

Abstract The microstructure of binary Co–13.6 wt% Cu and Cu–4.9 wt% Co alloys after long anneals (930–2,100 h) was studied between 880 and 1,085 °C. The contact angles between (Co) particles and (Cu)/(Cu) grain boundaries (GBs) in the Cu–4.9 wt% Co alloy are between 50° and 70°. In the Co–13.6 wt% Cu alloy, the transition from incomplete to complete wetting (coverage) of (Co)/(Co) GBs by the second solid phase (Cu) has been observed. The portion of completely wetted (Co)/(Co) GBs increases with increasing temperature beginning from $T_{\text{wss}} = 970 \pm 10$ °C and reaches a maximum of 15% at 1,040 °C. This temperature is very close to the Curie point in the Co–Cu alloys (1,050 °C). Above 1,040 °C, the amount of completely wetted (Co)/(Co) GBs decreases with increasing temperature and reaches zero at $T_{\text{wsf}} = 1,075 \pm 5$ °C. Such reversible transition from incomplete

to complete wetting (coverage) of a GB by a second solid phase is observed for the first time.

Introduction

The equilibrium and reversible transition from incomplete to complete wetting of grain boundaries (GBs) by the liquid phase (melt) has been experimentally observed in a numerous systems like Zn–Sn, Ag–Pb, Al–Cd, Al–In, Al–Pb, W–Ni, W–Cu, W–Fe, Mo–Ni, Mo–Cu, Mo–Fe, Cu–In, Al–Sn [1–5]. The formation of continuous layers of a liquid phase between solid grains is broadly used, particularly in various technological processes like liquid-phase sintering, welding or soldering. Recently, it has been observed in the Zn–Al and Al–Mg alloys that similar GB wetting transition can proceed even in case when a second phase wetting GBs is solid [6, 7]. In order to mark a difference with the GB wetting by a liquid phase, it can be called a GB coverage transition. There are good reasons to expect that the complete wetting (coverage) of GBs by a second solid phase can be observed in many technologically important systems, particularly in the Co–Cu alloys. They are broadly used for the electronic applications and are especially promising due to their giant magnetoresistance [8]. Therefore, the possibility of the formation of equilibrium GB layers of a second solid phase as well as the values of equilibrium contact angles in the triple joints between a GB and two interphase boundaries are very important. Also, the probability to observe the GB wetting (coverage) by a second solid phase is quite high in the Co–Cu alloys, since liquid Cu almost completely wets the surface of Co single crystals and polycrystals at 1,122 °C (i.e. slightly above the peritectic temperature, Fig. 1) and can completely wet the GBs [9, 10].

B. B. Straumal (✉) · O. A. Kogtenkova ·
A. B. Straumal · Yu. O. Kucheyev
Institute of Solid State Physics Russian Academy of Sciences,
Chernogolovka 142432, Russia
e-mail: straumal@issp.ac.ru; straumal@mf.mpg.de

B. B. Straumal · Yu. O. Kucheyev
Max-Planck Institut für Metallforschung, Heisenbergstraße 3,
70569 Stuttgart, Germany

A. B. Straumal · Yu. O. Kucheyev
National University of Research and Technology “MISiS”,
Leninsky Prospect 4, 119991 Moscow, Russia

B. Baretzky
Karlsruhe Institute for Technology (KIT), Institute for
Nanotechnology, Hermann-von-Helmholtz-Platz 1, 76344
Eggenstein-Leopoldshafen, Germany

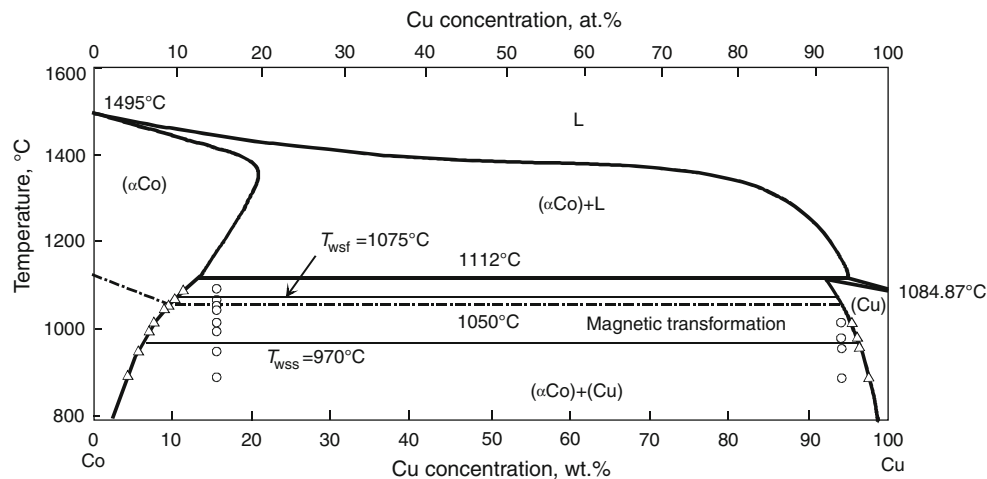


Fig. 1 Part of the Co–Cu phase diagram. *Thick lines* denote the bulk phase transitions and are taken from Ref. [11]. *Circles* denote the points where the Co–Cu alloys were annealed. *Triangles* denote the measured concentration in the (Co) and (Cu) solid solutions. *Thin*

lines at $T_{wss} = 970$ °C and $T_{wsf} = 1,075$ °C denote the tie-lines of the start and finish of the GB wetting (coverage) phase transition of (Co)/(Co) GBs by the second solid phase (Cu), respectively

Experimental

The Co–13.6 wt% Cu and Cu–4.9 wt% Co alloys (Fig. 1) were prepared from the high-purity 5N Cu and Co by a vacuum induction melting in a form of cylindrical ingots. The 2-mm thick slices were cut from the \varnothing 10 mm cylindrical Co–Cu ingots perpendicular to the ingot axis, and each sample was sealed into evacuated silica ampoule with a residual pressure of approximately 4×10^{-4} Pa at room temperature. Samples were annealed at temperatures between 880 and 1,085 °C (see experimental points in the Co–Cu phase diagram, Fig. 1) during long time (between 2,100 h at 880 °C and 930 h at 1,085 °C), and then quenched in water. The accuracy of the annealing temperature was ± 2 °C. After quenching, samples were embedded in resin and then mechanically ground and polished, using 1 μ m diamond paste in the last polishing step, for the metallographic study. After etching, samples were investigated by means of the light microscopy and scanning electron microscopy (SEM). SEM investigations were carried out in a Tescan Vega TS5130 MM microscope equipped by the LINK energy-dispersive spectrometer produced by Oxford Instruments. Using the same equipment, the composition of various structural elements in the annealed and quenched samples was controlled with the aid of electron probe microanalysis. Light microscopy has been performed using Neophot-32 light microscope equipped with 10 Mpix Canon Digital Rebel XT camera. A quantitative analysis of the wetting (coverage) transition was performed adopting the following criterion: every (Co)/(Co) GB was considered to be completely wetted only when a layer of (Cu) solid solution had covered the whole GB; if such a layer appeared to be interrupted, the GB was

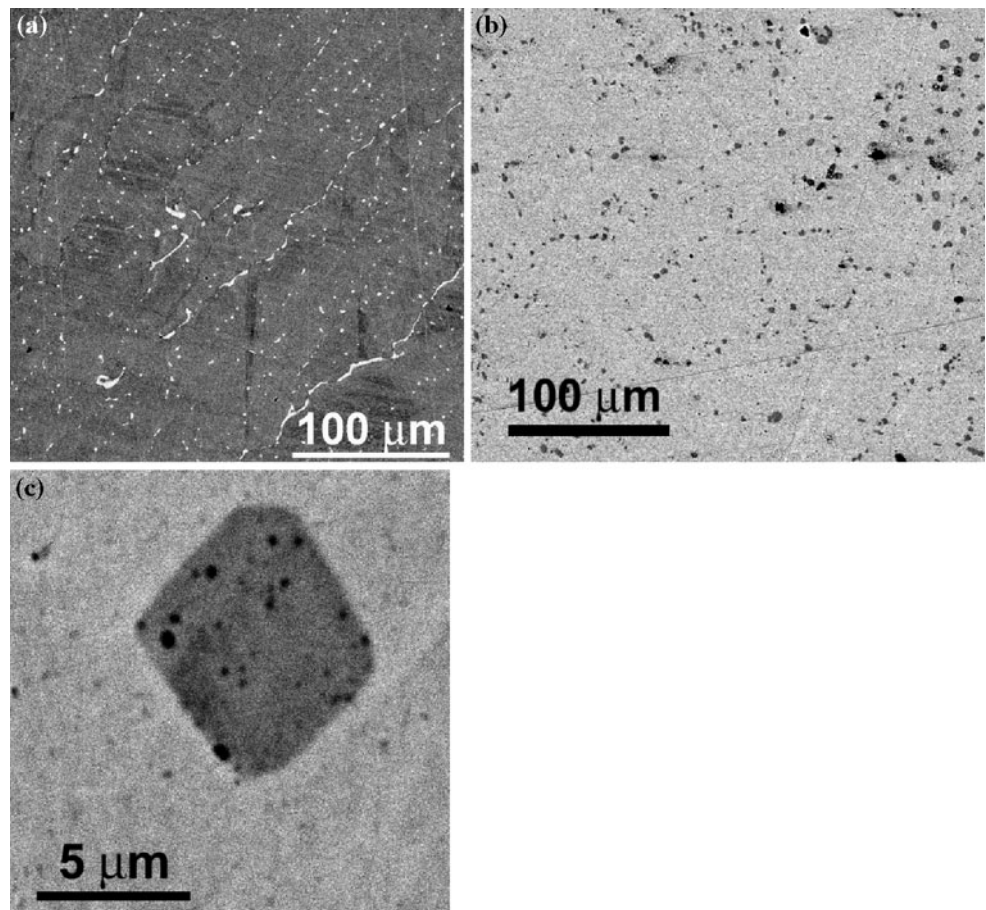
regarded as a partially wetted. In case of partially wetted (Co)/(Co) GBs, the contact angle between (Co)/(Co) GB and (Cu) solid solution was measured. In case of partially wetted (Cu)/(Cu) GBs, the contact angle between (Cu)/(Cu) GB and (Co) solid solution was measured. At least 100 GBs were analysed at each temperature. Typical micrographs obtained by SEM are shown in Fig. 2.

Results and discussion

SEM micrographs of the Co–Cu alloys annealed at 1,040 °C, 1,460 h are shown in Fig. 2. In the Co–13.6 wt% Cu alloy (Fig. 2a), both completely and incompletely wetted (Co)/(Co) GBs are visible. The grains of the Co-based solid solution appear dark-grey. The particles of the (Cu) solid solution phase (appears light-grey) form chains along the incompletely wetted (Co)/(Co) GBs (Fig. 2a). Some (Co)/(Co) GBs are completely wetted by (Cu). In this case, the (Cu) solid solution forms the continuous layer separating the (Co) grains. Before the annealing, the Co–13.6 wt% Cu samples had a typical cast microstructure, i.e. the elongated grains grown radially from the surface towards the ingot axis in the ingot periphery and the equiaxial grains in the ingot core, in the cylindrical area around its axis with diameter about 1 mm. This grain structure almost did not change during the long annealings of Co–13.6 wt% Cu samples, the radial grains are visible in Fig. 2a, they are aligned along its diagonal.

In the Cu–4.9 wt% Co alloy, the (Cu) grains are equiaxed. They have a size around 50–70 nm and are not elongated. This indicates possible evolution of the cast structure during the annealing (like for example in the work

Fig. 2 SEM micrographs of the annealed Co–Cu alloys: **a** Co–13.6 wt% Cu alloy (1,040 °C, 1,460 h), **b** Cu–4.9 wt% Co alloy (960 °C, 1,600 h), **c** faceted (Co) particle in the bulk Cu–4.9 wt% Co alloy (1,040 °C, 1,460 h). The Co-based solid solution grains appear *dark-grey* (matrix in the Co-rich alloy and particles in the Cu-rich alloy). The grains of Cu-based solid solution appear *light-grey* (matrix in the Cu-rich alloy and particles in the Co-rich alloy)



devoted to the investigation of GB wetting (coverage) in the Ni–Pb alloys [12]). In the Cu–4.9 wt% Co alloy only the chains of very fine (Co) particles are present in (Cu)/(Cu) GBs (Fig. 2b). The isolated (Co) particles in the bulk are large in comparison with GB particles and strongly faceted (Fig. 2b). These circumstances allow only rough estimation of the contact angle between (Cu)/(Cu) GBs and (Co) particles, it is nearly 50°–70°. In any case, no (Cu)/(Cu) GBs completely wetted by the (Co) solid phase were observed at all studied temperatures.

In Fig. 3, the temperature dependence for the fraction of (Co)/(Co) GBs completely wetted by the (Cu) phase (full circles, thin line) and for the mean contact angle between (Co)/(Co) GBs and the (Cu) phase (open circles, thick line) is shown. We calculated the mean contact angle since the polycrystal contains various GBs with different energy (depending on the GB misorientation and inclination). Same is true also for the energy of (Co)/(Cu) interphase boundaries. At 885 °C, only (Co)/(Co) GBs partially wetted by the (Cu) phase are present. At 985 °C, few (Co)/(Co) GBs completely wetted by the (Cu) phase appear. It means that the starting temperature of the GB wetting (coverage) phase transition of (Co)/(Co) GBs by the second solid phase (Cu) can be estimated as $T_{wss} = 970 \pm 10$ °C.

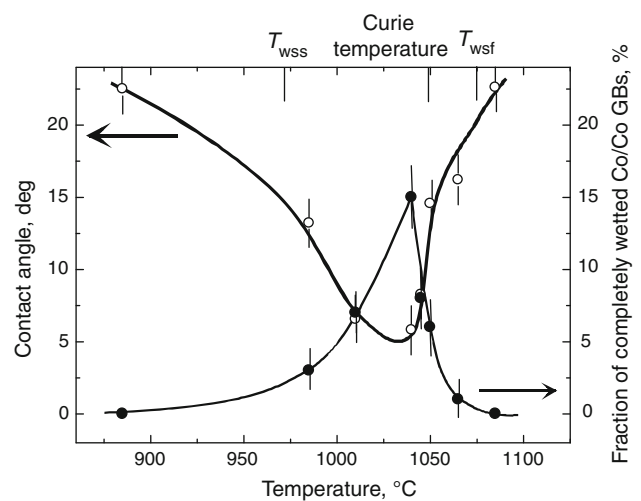


Fig. 3 Temperature dependence for the fraction of (Co)/(Co) GBs completely wetted by the (Cu) phase (full circles, thin line) and for the mean contact angle between (Co)/(Co) GBs and the (Cu) phase (open circles, thick line)

Above 985 °C, the amount of completely wetted (Co)/(Co) GBs increases with increasing temperature and reaches a maximum of about 15% at 1,040 °C. Above 1,040 °C, the amount of completely wetted (Co)/(Co) GBs decreases

with increasing temperature. At 1,065 °C, only about 1% (Co)/(Co) GBs are completely wetted. At 1,085 °C, no completely wetted (Co)/(Co) GBs could be found in the Co–13.6 wt% Cu polycrystal. It means that the finish temperature of the GB wetting (coverage) phase transition of (Co)/(Co) GBs by the second solid phase (Cu) can be estimated as $T_{\text{wsf}} = 1075 \pm 5$ °C. As a result, two new tie-lines at $T_{\text{wss}} = 970$ °C and $T_{\text{wsf}} = 1075$ °C appear in the two-phase area of the Co–Cu bulk phase diagram (Fig. 1). The mean contact angle (Fig. 3) first decreases with increasing temperature and reaches a minimum of about $6 \pm 2^\circ$ at 1,040 °C. Above 1,040 °C, the mean contact angle increases with increasing temperature and reaches a value of $22 \pm 2^\circ$ at 1,085 °C. At 1,040 °C, both the contact angle reaches a minimum and the amount of completely wetted (Co)/(Co) GBs becomes maximal.

Thin equilibrium GB or surface films were first considered by Cahn [13] and Ebner and Saam [14]. They proposed the idea that the transition from incomplete to complete surface wetting is a phase transformation. Cahn also analysed the case when wetting phase is solid [15]. Later the idea of wetting transformations was successfully applied for GBs, also old data on GB wetting were reconsidered from this point of view [3–5]. The phenomenon of the transition from incomplete to complete wetting is more general than the wetting under the consolute point originally proposed by Cahn [13, 15] and analysed further in numerous works [16, 17]. The modified Cahn's model was developed based on the numerous experimental results [18]. The transition from incomplete to complete wetting occurs in all systems where the temperature dependences of interface energies intersect [18]. In particular, GB wetting phase transformation proceeds at the temperature T_w where GB energy σ_{GB} becomes equal to the energy $2\sigma_{\text{SL}}$ of two solid/liquid interfaces. Above T_w , GB is substituted by a layer of the melt. The tie-line of the GB wetting phase transition appears in the two-phase area of a bulk phase diagram. For example, in the (Al) + L two-phase region of the Al–Zn system, the GB transformation for the Al/Al GBs wetting by Zn-containing melt occurs [19]. The completely wetted GBs in the Al–Mg polycrystals do not exist below $T_{\text{wmin}} = 440$ °C. T_{wmin} is the wetting temperature for a GB with maximal energy σ_{GBmax} . Above $T_{\text{wmax}} = 565$ °C, all high-angle GBs in (Al) are completely wetted by the melt [19]. T_{wmax} is the wetting temperature for a GB with minimal energy σ_{GBmin} . GBs can also be “wetted” (covered) by a second solid phase, as we can see in this work, too [15, 17]. The reversible transition from incomplete to complete solid phase wetting (coverage) was observed for the first time in the Zn–Al system and later also in the Al–Mg system [7, 8].

Following the Cahn's generic phase diagram, the more sophisticated theories of GB phases, segregation and

wetting layers were developed [16–18]. Thin films of interfacial phases were observed in GBs in metals (works of Luo and coworkers [20–22]), in oxides ([23], see also concept of complexions by Harmer et al. [24–28]), in interphase boundaries (Kaplan with coworkers [29–31]). According to those developments, the GB wetting tie-lines continue as prewetting (or GB solidus or solvus) lines in the one-phase (Al) area. Such GB solvus lines should exist also in the Co–Cu system because the (Co)/(Co) GBs completely wetted by the (Cu) phase are observed between $T_{\text{wss}} = 970$ °C and $T_{\text{wsf}} = 1,075$ °C.

The GB solidus lines were first observed in the early works on the GB Zn diffusion in the bicrystals of Fe–Si alloys [32–35]. GBs between GB solidus and bulk solidus possessed the high Zn diffusivity. In particular, in the Fe–5 at.% Si alloys, close to the intersection of the GB solidus line with the line of Curie transformation, the GB solidus has a pronounced ‘nose’ towards low Zn concentration [32]. In this work, we observe that the portion of (Co)/(Co) GBs wetted by solid (Cu) increases with decreasing temperature above Curie point (i.e. in the paramagnetic region). However, below Curie point when Co becomes ferromagnetic, the portion of (Co)/(Co) GBs wetted by solid (Cu) start to decrease with decreasing temperature. It continuously decreases parallel to the increasing of Co magnetization. It has been shown in [32] that below the Curie point the additional attractive force appears between two ferromagnetic grains separated by the wetting (coverage) layer of a diamagnetic or paramagnetic phase (remember that if a magnet is cut in two parts, the fragments attract one another). This attractive force increases with decreasing temperature according to the Curie–Weiss law and can destroy the conditions of complete wetting. Most probably, this effect is observed in our experiments in the Co–Cu alloys. In addition, we have to underline that the GB solidus lines should exist in the one-phase (Co) region in the Co–Cu bulk phase diagram between $T_{\text{wss}} = 970$ °C and $T_{\text{wsf}} = 1075$ °C (similar to the Al–Zn [19, 36, 37], Cu–Bi [38–41] and W–Ni [21, 22] systems).

In summary, the GB wetting (coverage) phase transition proceeds in the Co-rich alloys and does not proceed in the Cu-rich alloys in the Co–Cu system. The new GB tie-lines at $T_{\text{wss}} = 970$ °C and $T_{\text{wsf}} = 1,075$ °C appear in the Co–Cu phase diagram (Fig. 1). Between T_{wss} and T_{wsf} , some (Co)/(Co) GBs are completely wetted by the layers of solid (Cu) phase. The maximum portion of completely wetted (Co)/(Co) GBs is reached at 1,040 °C, i.e., close to the Curie point in the (Co) alloys.

Acknowledgements Authors thank the Russian Foundation for Basic Research (contracts 09-03-92481 and 09-03-00784), the Russian Federal Agency for Science and Innovations (contract 02.740.11.5081) and Israel Ministry of Science (project 3-5790) for the financial support. Authors cordially thank Prof. E. Rabkin,

Dr. A. Mazilkin and Dr. S. Protasova for stimulating discussions, Mr. A. Nekrasov for the help with SEM and EPMA measurements.

References

1. Passerone A, Eustathopoulos N, Desré P (1977) *J Less-Common Met* 52:37
2. Passerone A, Sangiorgi R, Eustathopoulos N (1982) *Scr Metall* 16:547
3. Eustathopoulos N (1983) *Int Met Rev* 28:189
4. Straumal BB (2003) Grain boundary phase transitions. Nauka publishers, Moscow in Russian
5. Straumal B, Molodov D, Gust W (1995) *Interface Sci* 3:127
6. López GA, Mittemeijer EJ, Straumal BB (2004) *Acta Mater* 52:4537
7. Straumal BB, Baretzky B, Kogtenkova OA, Straumal AB, Sidorenko AS (2010) *J Mater Sci* 45:2057. doi:10.1007/s10853-009-4014-6
8. Errahmani H, Berrada A, Schmerber G, Dinia A (2002) *J Magn Magn Mater* 238:145
9. Kolbe M, Brillo J, Egry I, Herlach D, Ratke L, Chatain D, Tinet N, Antion C, Battezzati L, Curiotto S, Johnson E, Pryds N (2006) *Microgravity Sci Technol* 18:174
10. Curiotto S, Chatain D (2009) *Scr Mater* 60:40
11. Massalski TB (ed) (1990) Binary alloy phase diagrams, 2nd edn. ASM International, Materials Park, OH
12. Bernardini J, Monchoux J-P, Chatain D, Rabkin E (2002) *J Phys IV France* 12:Pr8
13. Cahn JW (1977) *J Chem Phys* 66:3667
14. Ebner C, Saam WF (1977) *Phys Rev Lett* 38:1486
15. Cahn JW (2000) *Physica A* 279:195
16. Wynblatt P, Saul A, Chatain D (1998) *Acta Mater* 46:2337
17. Wynblatt P, Chatain D (2008) *Mater Sci Eng A* 495:119
18. Bishop CM, Tang M, Cannon RM, Carter WC (2006) *Mater Sci Eng A* 422:102
19. Straumal BB, Gornakova AS, Kogtenkova OA, Protasova SG, Sursaeva VG, Baretzky B (2008) *Phys Rev B* 78:054202
20. Luo J (2008) *Curr Opin Solid State Mater Sci* 12:81
21. Gupta VK, Yoon DH, Meyer HM et al (2007) *Acta Mater* 55:3131
22. Luo J, Gupta VK, Yoon DH et al (2005) *Appl Phys Lett* 87:231902
23. Luo J, Chiang Y-M (2008) *Ann Rev Mater Res* 38:227
24. Luo J, Dillon SJ, Harmer MP (2009) *Microsc Today* 17:22
25. Cho J, Wang CM, Chan HM, Rickman JM, Harmer MP (2002) *J Mater Sci* 37:59. doi:10.1023/A:1013185506017
26. Dillon SJ, Tang M, Carter WC, Harmer MP (2007) *Acta Mater* 55:6208
27. Dillon SJ, Harmer MP (2007) *Acta Mater* 55:5247
28. Dillon SJ, Harmer MP (2008) *J Eur Ceram Soc* 28:1485
29. Baram M, Kaplan WD (2006) *J Mater Sci* 41:7775. doi:10.1007/s10853-006-0897-7
30. Sadan H, Kaplan WD (2006) *J Mater Sci* 41:5099. doi:10.1007/s10853-006-0437-5
31. Levi G, Kaplan WD (2006) *J Mater Sci* 41:817. doi:10.1007/s10853-006-6565-0
32. Rabkin EI, Semenov VN, Shvindlerman LS et al (1991) *Acta Metall Mater* 39:627
33. Noskovich OI, Rabkin EI, Semenov VN et al (1991) *Acta Metall Mater* 39:3091
34. Straumal BB, Noskovich OI, Semenov VN et al (1992) *Acta Metall Mater* 40:795
35. Straumal B, Rabkin E, Lojkowski W et al (1997) *Acta Mater* 45:1931
36. Straumal BB, Mazilkin AA, Kogtenkova OA et al (2007) *Philos Mag Lett* 87:423
37. Straumal B, Valiev R, Kogtenkova O et al (2008) *Acta Mater* 56:6123
38. Divinski SV, Lohmann M, Herzig Chr et al (2005) *Phys Rev B* 71:104104
39. Chang L-S, Rabkin E, Straumal BB et al (1999) *Acta Mater* 47:4041
40. Straumal BB, Polyakov SA, Chang L-S et al (2007) *Int J Mater Res* 98:451
41. Straumal B, Prokofjev SI, Chang L-S et al (2001) *Defects Diffus Forum* 194:1343